A Hexameric Helicase Encircles One DNA Strand and Excludes the Other during DNA Unwinding†

Kevin J. Hacker and Kenneth A. Johnson*

Department of Biochemistry and Molecular Biology, 106 Althouse Laboratory, The Pennsylvania State University, University Park, Pennsylvania 16802

Received July 8, 1997; Revised Manuscript Received September 12, 1997⊗

ABSTRACT: The bacteriophage T7 DNA helicase/primase (gene 4 protein) is a ring-like hexamer that encircles ssDNA and requires forked DNA to catalyze DNA unwinding. We report that optimal rates of unwinding of forked DNA require ssDNA tails of 55 nucleotides on the 5′-to-3′ strand and 15 nucleotides on the 3′-to-5′ strand. Surprisingly, streptavidin bound to a biotinylated 3′-end fully substitutes for the 3′-to-5′ ssDNA tail. This suggests that excluding the 3′-to-5′ DNA strand from the center of the helicase is an essential aspect of the mechanism of hexameric helicase-catalyzed DNA unwinding. We also report that streptavidin bound to a biotinylated dT within the 5′-to-3′ strand of the duplexed region abolishes DNA unwinding; whereas, streptavidin bound to a biotinylated dT within the duplexed region of the other strand has no effect. These results unambiguously demonstrate that the T7 gene 4 protein is a 5′-to-3′ helicase and imply that during DNA unwinding the 5′-to-3′ strand transverses the center of the ring while the 3′-to-5′ strand is excluded from the center of the ring. Implications for collisions between a helicase and other protein−DNA complexes are discussed.

Helicases couple the hydrolysis of nucleoside 5′-triphosphates to the transient unwinding of duplex (ds)[1] DNA—an essential step in almost all aspects of DNA metabolism (i.e., DNA replication, recombination, and repair) (*1, 2*). An increasing number of helicase-related diseases have been identified, reflecting their involvement in a great number of diverse cellular processes (*3*−*6*). Our understanding of the cell or these diseases will not be satisfactory until the mechanism of helicase-catalyzed DNA unwinding is understood. While a detailed analysis of the dimeric *Rep* helicase of *Escherichia coli* has been presented and a model for its mechanism proposed, no ring-like hexameric DNA helicase, which drives genomic DNA replication in most cells, is understood in detail (*7*). We have used the T7 gene 4 DNA helicase as a model protein for studying these helicases, which have many properties in common.

The bacteriophage T7 gene 4 protein is an essential T7 enzyme that catalyzes both the unwinding of DNA and the synthesis of primers required for T7 DNA replication (*8, 9*). The T7 gene 4 encodes two collinear polypeptides of 56 and 63 kDa molecular mass; the smaller 56-kDa protein is generated from a second internal ribosomal binding site (*10*). The 63-kDa polypeptide has both primase and helicase activities; whereas, the 56-kDa protein lacks primase activity (*2*). Biochemical and electron microscopy (EM) studies have shown that the helicase is hexameric and ring-like in structure with D_6 symmetry—roughly similar to hexameric helicases: *E. coli Ruv*B protein, *E. coli Rho*, and T4 phage gene 41 helicases (*11*−*15*). The T7 DNA helicase is unusual in that TTP is the preferred nucleotide (*8, 16, 17*). However, the TTP binding site is structurally related to that of the ATP binding sites of *E. coli Rho*, *E. coli Rec*A, and F_1-ATPase at least at the level of primary sequence (*18, 19*). While the DNA was not directly visualized in EM studies, image analysis suggests that the helicase encircles the ssDNA (*11, 14*).

Like most hexameric helicases, the T7 gene 4 DNA helicase requires both 5′- and 3′-ssDNA tails attached to the duplex DNA (i.e., forked DNA) to initiate unwinding (*2, 7*). The requirement for forked DNA is a major difference between the hexameric T7 DNA helicase and the well-characterized dimeric *E. coli Rep* helicase, which requires only a 3′-to-5′ ssDNA tail to initiate DNA unwinding (*20*). This difference may reflect different general mechanisms of DNA unwinding by the two proteins. The T7 DNA helicase will unwind a DNA substrate that resembles a replication fork with a 3′-tail greater than 6−7 nucleotides and a 5′-ssDNA tail greater than 13 nucleotides (*8*). Whether both of these tails traverse the center of the helicase is unknown. Since both ssDNA tails are required, the supposed direction of T7 helicase-catalyzed DNA unwinding is unclear. The direction of DNA unwinding is normally presumed to be defined by the polarity of the ssDNA tail (5′ or 3′) required at the ss/dsDNA junction for unwinding to occur. Therefore, the only evidence indicating the direction of T7 DNA helicase DNA unwinding is based on the finding that primers are laid down in the 5′-to-3′ direction along a M13 ssDNA molecule (*9*). However, these results are complicated by intramolecular duplex DNA that can form on a M13 DNA molecule. Thus, while the helicase is thought to unwind DNA in the 5′-to-3′ direction as it moves along the lagging strand of the replication fork (*9*), this fundamental aspect of the T7 DNA helicase mechanism and that of many other helicases requiring both ssDNA tails is not known conclusively.

† This work was supported by a grant from the National Institutes of Health (GM44613) to K.A.J. and an American Cancer Society postdoctoral fellowship (PF-4024) to K.J.H.

* Author to whom correspondence should be addressed. Fax: 814-865-3030.

⊗ Abstract published in *Advance ACS Abstracts,* November 1, 1997.

[1] Abbreviations: ssDNA, single-stranded DNA, dsDNA, double-stranded DNA.

S0006-2960(97)01644-9 CCC: $14.00 © 1997 American Chemical Society

We have varied the length of the ssDNA tails and used novel streptavidin-bound biotinylated DNA substrates to address the following fundamental questions: (a) Does the ssDNA interact with more than one subunit of the helicase at one time during DNA unwinding? (b) Does the helicase interact with one or both of the ssDNA tails? (c) Do one or both of the ssDNA tails travel through the center of the helicase ring during DNA unwinding? On the basis of our findings, we have ruled out several models for the mechanism of helicase-catalyzed DNA unwinding and propose a possible mechanism.

EXPERIMENTAL PROCEDURES

Materials. The chemicals and where they were purchased are as follows: radioactive ATP, ICN; TTP, U.S. Biochemical Corp.; acetylated BSA, Gibco-BRL; streptavidin and biotin, Sigma; T4 polynucleotide kinase, New England Biolabs; polyacrylamide, Bio-Rad Laboratories. Recombinant streptavidin, Stv13, was a generous gift from Dr. Takeshi Sano, Boston University. All oligonucleotides were synthesized by Integrated DNA Technologies, Coralville, IA, except 3′-biotinylated terminus oligonucleotide, which was synthesized at Operon, TX. The 63-kDa T7 DNA helicase/primase was purified according to Patel et al. (*17*).

Helicase buffer is 50 mM sodium acetate, 50 mM Tris acetate (pH 7.5 at 23 °C), 10 mM magnesium acetate, 1 mM dithiothreitol, and 100 mg/mL acetylated bovine serum albumin.

DNA Substrates. Oligonucleotides were purified by electrophoreses through a denaturing polyacrylamide gel, isolated by the crush−soak method (*21*), and desalted by passage through a Sep-Pak C_{18} column according to manufacturer's instructions (Waters Corporation). The 5′-end labeling of oligonucleotides with ^{32}P was performed using T4 polynucleotide kinase under standard conditions (*21*). Polynucleotide kinase was removed by phenol extraction, and unincorporated ^{32}P was removed by passage through a Biospin-6 column according to the manufacturer's instructions (Bio-Rad Laboratories). Oligonucleotides were annealed in 150 mM sodium acetate, 50 mM Tris acetate, pH 7.5, and 1 mM Na_3EDTA by incubation at 90 °C for 4 min followed by slow cooling to 30 °C.

Assay for the Effect of Helicase with TTP Preincubation on the Rate of DNA Unwinding Using Rapid Quench Technique. Reactions were carried out at 30 °C using the three-syringe, KinTec RQF-3 rapid quench-flow apparatus (State College, PA). Twice the final concentration of helicase (15 μL) was preincubated (with 1 mM TTP, where indicated) in helicase buffer in one loop of the quench-flow apparatus. The other loop contained 2 nM DNA molecules (twice the final concentration, 5′ ^{32}P end-labeled on the displaced strand) in helicase buffer and 2 mM TTP in reactions without helicase−TTP preincubation and 1 mM TTP with preincubation. Samples were incubated for at least 2 min in the loops at 30 °C. DNA unwinding by the helicase was initiated by rapid mixing of the solutions and stopped by the addition of 0.3% sodium dodecyl sulfate (SDS)/13.3% (v/v) glycerol (final concentrations). Samples were electrophoresed on a 12% polyacrylamide/10 mM Tris borate, (pH 7.4), 1 mM Na_3EDTA (TBE) gel, and the amount of double-stranded and single-stranded DNA was quantified using a Betascope 603 blot analyzer (Betagen, Waltham, MA). The fraction of ssDNA molecules present at the start of the reaction (t_o) was determined from mock reactions performed without helicase. For each time point, the fraction of DNA unwound was calculated by subtracting the fraction of ssDNA present at t_o from the fraction of ssDNA observed and dividing by the fraction of duplex DNA at t_o. The plot of DNA unwound versus time was fit to the following equation: fraction of DNA unwound $= A(1 - e^{(-k_1 t)}) + k_2 t$ when a lag was not observed, and fit to the double exponential equation: fraction of DNA unwound $= A\{1 + (1/k_1 + k_2)[k_2\, e^{(-k_1 t)} - k_1 e^{(-k_2 t)}]\}$ when a lag was observed, where A is the amplitude of DNA unwinding, and k_1 and k_2 are rate constants for DNA unwinding. All fits to the data were both performed by nonlinear least squares analyses and plotted using Kaleidagraph (Synergy Software, Reading, PA).

Optimal 5′- and 3′-ssDNA Tail Determination. Reactions were performed in a circulating water bath at 8 °C. Helicase buffer was adjusted to be pH 7.4 at 8 °C. 1 nM DNA substrate (5′ ^{32}P end-labeled on the displaced strand) and 1 mM TTP (final concentrations) in 20 μL of helicase buffer were added to 5 μL of helicase and 1 mM TTP in helicase buffer, which was preincubated in an ice water bath for at least 5 min prior to mixing. DNA unwinding was stopped with 100 μL of 1% SDS (w/v), 0.1 M Na_3EDTA, 6% glycerol (v/v), 50 mM Tris acetate, pH 7.5, and marker dyes at room temperature (21−23 °C). Samples were immediately removed from the 8 °C circulating water bath and placed at room temperature to prevent precipitation of the SDS. Samples were electrophoresed through a 8% polyacrylamide/TBE gel and analyzed as described above.

Assay for the Effect of Streptavidin-Biotinylated DNA on Helicase Activity. Where the presence of streptavidin is indicated, streptavidin was added in 50-fold excess (tetramer) over DNA (50:1 nM) and allowed to incubate with the DNA for at least 5 min prior to adding helicase. Reactions with the 3′-biotinylated end were performed as described for nonbiotinylated DNA except samples were electrophoresed through a 6% polyacrylamide/TBE gel.

DNA substrates with biotin-dT in the duplexed region were performed as described above with the following exceptions: (a) DNA substrates were added to a helicase/TTP solution containing 40 000-fold excess biotin (40 μM) to prevent rebinding of any streptavidin displaced from DNA. (b) Recombinant streptavidin, Stv13, which has eight amino acid residues deleted (*22*), was used. The switch from natural streptavidin to Stv13 enabled us to separate streptavidin-bound ssDNA from free dsDNA on 6% polyacrylamide/TBE gels. (c) Reactions were performed in a circulating water bath at 18 °C (the maximum temperature where the rate of DNA unwinding could still be measured accurately by initiating and stopping reactions by hand). (d) For reaction of less than 10 s, timing was accomplished with the aid of a metronome (Seiko).

RESULTS

At Low T7 DNA Helicase Concentration, Preincubation of the Helicase with TTP Removes an Early Lag before the Onset of Rapid DNA Unwinding. As a prerequisite for our studies of helicase-catalyzed unwinding of a variety of DNA substrates, we determined the effect of helicase preincubation with TTP on the rate of DNA unwinding. During the preincubation and after mixing the helicase with DNA, the

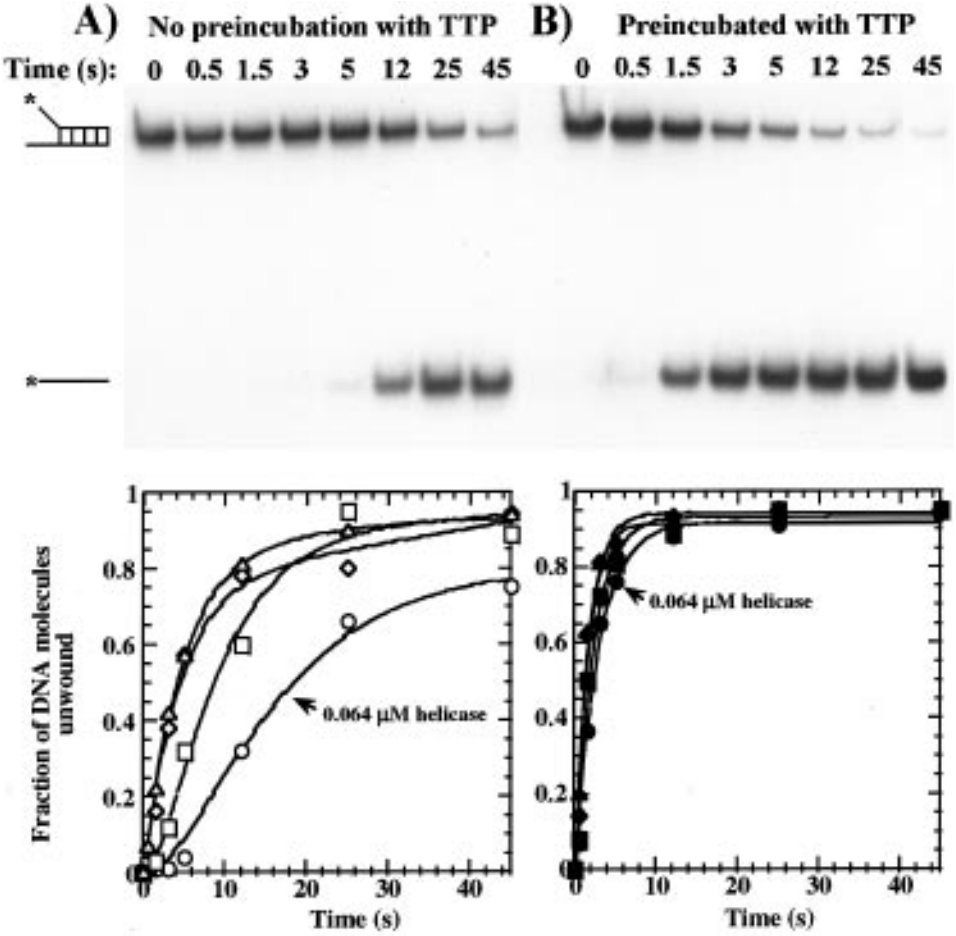

FIGURE 1: Effect of helicase preincubation with TTP on the onset of rapid DNA unwinding. Without (A) and with (B) prior incubation with TTP the T7 DNA helicase was rapidly mixed with DNA substrate and TTP to initiate DNA unwinding. Reactions were carried out at 30 °C with DNA substrate III in Table 1, which consists of a 35-bp duplex, defined 40 nucleotide 3′-ssDNA tail, and a $(dT)_{35}$ 5′-tail. At the top of the figure, an image of the 0.064 μM (monomer) helicase samples electrophoresed on a 12% polyacrylamide/TBE gel is shown. The amount of double-stranded DNA versus displaced ssDNA was quantified using a Betascope, MA, and a plot of the results is shown at the bottom of the figure (circles, marked with arrows). The plot also shows the results of reactions with helicase concentrations of 0.127 μM (squares), 0.38 μM (diamonds), and 1.14 μM (triangles) without [(A) open symbols] and with [(B) shaded symbols] prior incubation with TTP. The data were fit to single and double exponential equations, and the best fit is shown.

TTP concentration (1 mM) was at saturating levels. The DNA substrate was kept very low (1 nM) in our studies to eliminate reannealing of the unwound DNA that can occur at higher DNA concentrations. Under these low DNA concentrations, the helicase was always in vast excess over DNA.

In the absence of helicase preincubation with TTP, at the lowest concentration of helicase studied (0.064 μM monomer), a 5 s lag precedes the onset of rapid DNA unwinding (Figure 1A, top of figure and marked with arrows in the plot). As the helicase concentration is increased to 0.38 μM, the lag is nearly eliminated.

When the helicase was preincubated with TTP, no lag was observed even at the lowest concentration of helicase studied (0.064 μM) (Figure 1B). Interestingly, at the highest concentration of helicase studied (1.14 μM), the rate of DNA unwinding is more than 3-fold faster than that rate seen at 1.14 μM helicase in the absence of TTP preincubation (0.68 $\pm$ 0.07 and 0.21 $\pm$ 0.01 DNA molecules/s, respectively).

The lag seen at low helicase concentrations in the absence of TTP most likely represents a slow nucleotide-dependent assembly of the helicase subunits into the active ring-like hexameric form. These results suggest that assembly of the hexameric form is partially rate limiting and only the assembled hexamer binds to the DNA. As suggested for the *E. coli Dna*B and the T4 phage gene 41 helicases, this hexameric ring may exist in open and closed conformations that enable it to rapidly bind to and lock around the DNA (*23*, *24*). All of the following experiments were performed with the helicase preincubated with 1 mM TTP prior to initiating DNA unwinding.

Optimal ssDNA 5′-Tail Length Is Greater Than the Length of DNA Necessary To Travel through the Center of the Helicase. Matson et al. (*8*) determined the absolute minimum 5′ and 3′ ssDNA tail requirement for the helicase. We varied the length of the 5′-3′ ssDNA tail of a synthetic oligonucleotide (Table 1, substrate I) to determine the preferred tail length for DNA unwinding by the helicase. The helicase was at saturating levels in these experiments to limit any differences due to DNA binding alone (data not shown). To minimize thermal breathing of the DNA duplex, which would lead to an underestimate of the preferred ssDNA tail length, we performed the experiments at 8 °C. In addition, 5′-ssDNA tails consisting of poly(dT) ($(dT)_n$) were used to avoid possible intramolecular duplex DNA structures. Duplex DNA in the tail region would lead to an overestimate of the preferred ssDNA tail length. Figure 2 shows a plot of the results with DNA substrates with 5′-

Table 1: DNA Substrates

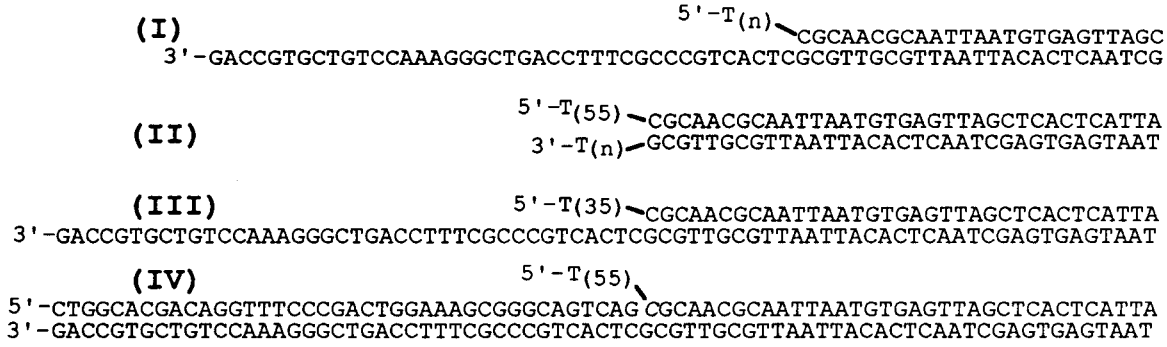

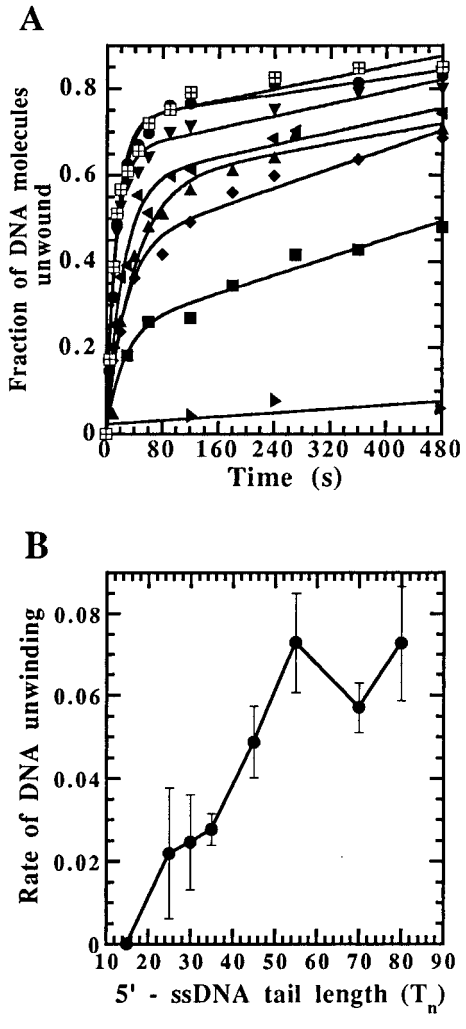

FIGURE 2: 5′-ssDNA tail length varied. Reactions were carried out at 8 °C with 0.9 μM helicase and DNA substrate I in Table 1. The DNA substrate I consists of 25 bp of the duplexed DNA, a defined 40 nucleotide 3′-ssDNA, and a 5′-poly(dT) tail as indicated. (A) A plot of the results of rapid mixing of the helicase (preincubated with TTP) with DNA substrates with increasing 5′-poly(dT) nucleotide chains [T_{15} (flags), T_{25} (squares), T_{30} (diamonds), T_{35} (triangles), T_{45} (reversed flags) T_{55} (inverted triangles), T_{70} (circles), and T_{80} (quartered box)] is shown. The data were fit to a single exponential equation, and the rate of DNA unwinding was determined. (B) A plot of the average rate of DNA unwinding as a function of the length of the 5′-ssDNA tail as determined from panel A and two additional repetitions of the experiment.

tails of 15, 25, 30, 35, 45, 55, 70, and 80 poly dT. A 5′-ssDNA tail of at least 55 nucleotides but less than 70 nucleotides is preferred. This range of tail length is significantly greater than the 29 nucleotides of ssDNA required to bind one subunit and travel through the center of the hexamer (*11*, *25*). This suggests that during DNA unwinding ssDNA is simultaneously bound by more than one helicase subunit in the hexamer. ssDNA may wrap around and contact all six subunits of the helicase (see Discussion).

A ssDNA 3′-Tail of 15 Nucleotides Is Enough for Rapid T7 DNA Helicase-Catalyzed DNA Unwinding. Efficient DNA Unwinding Is Also Observed if the 3′-Tail Is Fully Double-Stranded (i.e., a Nicked DNA Template). We determined the preferred 3′-to-5′ ssDNA tail length for DNA unwinding by the helicase essentially as described for the 5′-to-3′ ssDNA tail except a 35-base pair (bp) duplex DNA was used instead of a 25 bp (Table 1, substrate II). A plot of the results show that $(dT)_{15}$ ssDNA tail is sufficient for optimal rates of DNA unwinding (Figure 3).

The 0.029 s^{-1} rate of unwinding of a DNA molecule with a 40 nucleotide 3′-ssDNA tail containing all four nucleotides and defined in sequence (Table 1, substrate III) is within experimental error to the 0.02 s^{-1} T_{30} ssDNA tail rate (Figure 3, open circles). This 40-nucleotide tail was annealed with a complementary oligonucleotide of 40 nucleotides creating a nicked duplex with a 5′-ssDNA tail (Table 1, substrate IV). Surprisingly, the helicase unwinds this nicked DNA molecule at 0.032 s^{-1} (Figure 3, open squares); this rate is similar to the rate with a fully ssDNA 3′-tail. The data suggest that while a $(dT)_{15}$ ssDNA is sufficient for interacting with the helicase during DNA unwinding, a molecule that cannot fit in the center of the hexamer is also sufficient for a 3′-ssDNA end.

Streptavidin Bound to the Biotinylated 3′-End of the Duplex DNA Completely Substitutes for the 3′-ssDNA Tail Normally Required for DNA Unwinding by the Helicase. Streptavidin-biotinylated DNA was used to test our hypothesis that a molecule that cannot fit in the center of the hexamer would substitute for a 3′-ssDNA end flanking the duplex DNA. The streptavidin−biotin is ideal for preventing the 3′-end of the duplex from entering the center of the helicase. The 53.2-kDa streptavidin molecule binds with extremely high affinity to biotin ($K_d \sim 10^{-15}$) (*26*), and the 54-Å diameter of streptavidin is too large to fit in the 25−30-Å center of the helicase (*11*, *27*, *28*). The biotin moiety is attached to the 3′-nucleotide via a 15-atom "linker arm" such that streptavidin binding does not distort the DNA (*29*). In these experiments, DNA unwinding was initiated by the mixing of the helicase preincubated with TTP and DNA, which was first preincubated with streptavidin where indi-

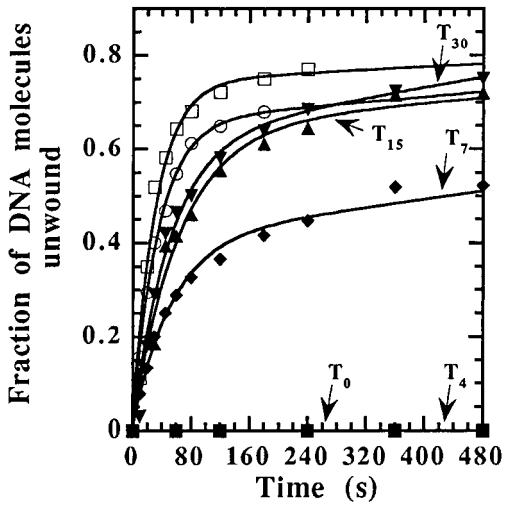

FIGURE 3: Length of 3′-ssDNA tail varied, and effect of a DNA molecule with fully double-stranded 3′-tail (nicked DNA with 5′-ssDNA tail) on DNA unwinding examined. Reactions were carried out at 8 °C with 0.9 μM helicase. DNA unwinding was initiated by adding helicase preincubated with TTP to the DNA. DNA substrate II defined in Table 1 was used, which consisted of the 35 bp of duplexed DNA, a 5′-$(dT)_{55}$ tail, and a 3′-tail as indicated. A plot of the results with DNA substrates containing no 3′-tail (closed circle) and 3′-tails of 4 (closed square), 7 (closed diamond), 15 (closed triangle), and 30 (closed inverted triangle) poly(dT) nucleotide chains is shown. Plotted also is the results employing DNA substrate III in Table 1, which contains a defined 3′-ssDNA tail of 40 nucleotides (open circle) and DNA substrate IV, which contains a fully duplexed 3′-tail obtained by annealing a 40 nucleotide oligonucleotide complementary to the 3′-tail of substrate III (open square).

cated. Figure 4A shows the results of reactions performed in the presence of streptavidin. Only those DNA molecules with a streptavidin bound to a biotin moiety at their 3′-end were unwound by the helicase. Biotinylated DNA used in the experiment was not purified free of those DNA molecules of the same sequence that lost the biotin moiety during their synthesis. These nonbiotinylated DNA molecules were easily separated from streptavidin-bound DNA by gel electrophoreses (see Figure 4A) and served as an internal control for the effect of free streptavidin on the helicase. As shown in Figure 4A, none of the duplex DNA molecules containing the nonbiotinylated oligonucleotides and therefore not bound by streptavidin were unwound by the helicase. Thus, free streptavidin does not effect helicase-catalyzed DNA unwinding.

A plot of the results in the presence (triangles) and absence (squares) of streptavidin and of a control forked DNA substrate (circles) is shown in Figure 4B. The streptavidin−biotin complex at the 3′-end of the DNA fully substitutes for the normally required 3′-ssDNA tail. This suggests that exclusion of the 3′-to-5′ polarity DNA strand from the center of the helicase is an important aspect of the mechanism of DNA unwinding by the helicase. This also confirms earlier studies that the helicase moves along the DNA of 5′-to-3′ polarity on the lagging strand during DNA replication (*9*, *30*).

Rather than spending our efforts examining the unlikely possibility that streptavidin could substitute for the 5′-end of the duplex DNA, we sought to confirm our interpretations of the results by examining the effect of streptavidin bound to a biotinylated nucleotide within the duplexed DNA.

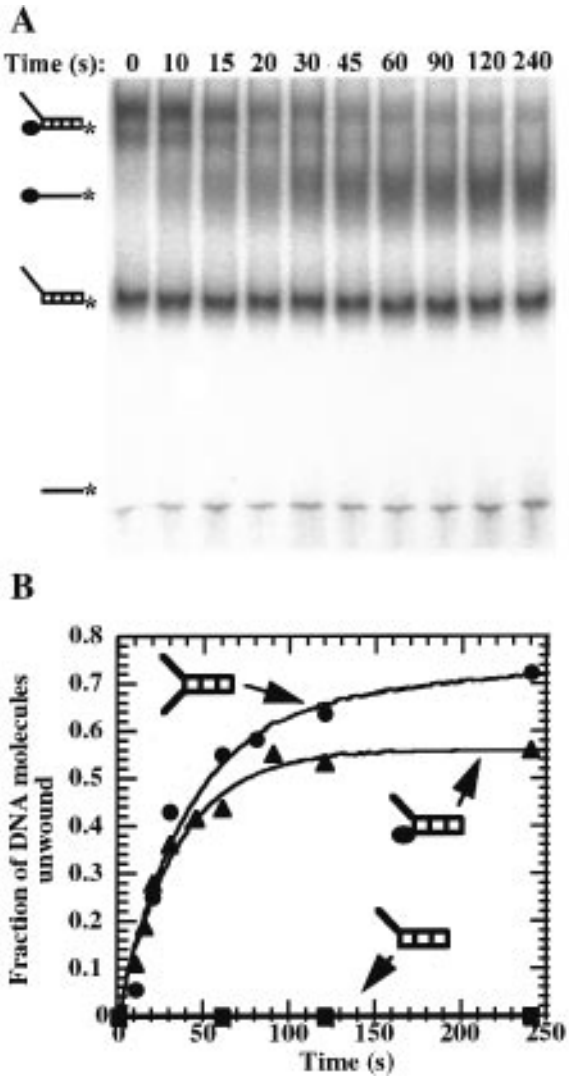

FIGURE 4: Effect of streptavidin bound to a 3′-biotinylated DNA end. 0.9 μM helicase (preincubated with TTP) was rapidly mixed with DNA substrate and TTP to initiate DNA unwinding. Reactions were carried out at 8 °C with DNA substrate II in Table 1 consisting of a 5′-tail of 55 poly(dT) nucleotides and 3′-tail or biotin as indicated. (A) Reactions with streptavidin (represented by a closed circle) and a mixture of DNA substrates with and without a biotin molecule covalently attached to their 3′-end strand and labeled with ^{32}P at their 5′-end were electrophoresed on a 12% polyacrylamide/TBE gel. An image of the gel is shown. The amount of double-stranded DNA bound with streptavidin versus displaced single-stranded DNA bound with streptavidin was quantified using a Phosphor Imager. (B) A plot of these results (triangle), the results without streptavidin present (square), and a control with the defined 3′-ssDNA tail of 40 nucleotides (circle; see Table 1 for oligonucleotide sequence) is shown. The results were fit to a single exponential equation, and the best fit is shown. The figures on the graph represent DNA molecules unwound by the helicase, and streptavidin is represented by a circle.

Streptavidin−Biotin Linked to the Duplexed Region of the Displaced Strand (3′-to-5′) Does Not Inhibit Helicase Action. While Streptavidin−Biotin Complex Linked to the 5′-to-3′ Strand Does Inhibit Helicase Action. To confirm that the 3′-to-5′ DNA strand is excluded from the center of the helicase while the 5′-to-3′ DNA travels through the center of the helicase during DNA unwinding, we examined the unwinding of DNA with a biotinylated dT in duplex DNA region either on the 5′-to-3′ or the 3′-to-5′ strand (Figure 5A). A similar experiment has been recently performed by Raney et al. (*31*) using the bacteriophage T4 gene 41 helicase

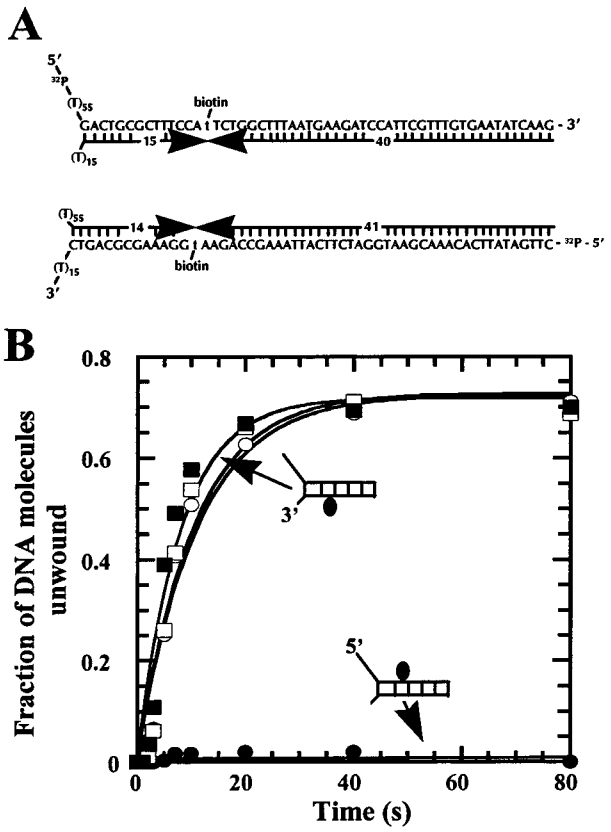

FIGURE 5: Effect of streptavidin bound to biotin covalently linked to a nucleotide in the duplexed region on the 5′-to-3′ or 3′-to-5′-DNA strand. (A) Diagram of the DNA molecules used in experiments with streptavidin is shown. All DNA molecules contained a 5′-$(dT)_{55}$ tail and a 3′-$(dT)_{15}$ tail. The nucleotide sequence of the DNA strand containing the biotinylated dT (represented by "t") is shown. It should be noted that the biotinylated DNA strands are complementary with each other. The arrowhead lines with hash marks represent the complementary DNA strand, which is not biotinylated, and the nucleotide distance from the beginning and end of the duplex DNA to the biotinylated dT are indicated on the arrowhead lines. (B) A plot of the results in the absence (open circles and squares) and presence of streptavidin (closed circles and squares) is shown. 5′-to-3′ and 3′-to-5′-biotinylated DNA are represented by circles and squares, respectively. In the graph, on figures representing DNA molecules, a shaded circle represents a biotinylated dT bound by streptavidin. Reactions were carried out at 18 °C with 0.22 μM helicase. DNA unwinding was initiated by adding helicase (preincubated with TTP) and excess biotin to the DNA.

and gene 59 protein. Our experimental design differs from that of Raney et al. (*31*) in two important ways. Raney et al used a BioTeg moiety for binding by streptavidin, which maintains regular spacing between the phosphate backbone of the DNA but does not contain a nucleoside and therefore may disrupt contacts required by the helicase during DNA unwinding. In contrast, we used a biotinylated dT nucleotide, which retains normal bp contacts. We also monitored the unwinding of the streptavidin-bound oligonucleotide in the presence of 40 000-fold excess biotin to trap any streptavidin displaced by the helicase. This control enabled us to rule out the possibility that our results could be due to the helicase being able to displace streptavidin bound to one DNA strand but not the other.

A longer length of duplex DNA (55 vs 35 bp) was chosen for these experiments to ensure that the streptavidin would encounter the center of the helicase during the unwinding of the DNA. The biotin moiety is attached to the C-6 of the dT base via a six-carbon linker. This places the biotin moiety in the major groove of the duplex DNA some 10 Å away from the base, and it is possible that the helicase could unwind the DNA many nucleotides beyond the biotinylated dT before encountering the bound streptavidin molecule. Therefore, the biotinylated dT was placed 40 bp away from the end of the duplex DNA to ensure contact between the helicase and the streptavidin before the DNA was nearly unwound. DNA unwinding reactions were stopped with the addition of SDS/EDTA, which dissassociates the helicase from the DNA and allows DNA molecules unwound only to the streptavidin-bound biotinylated dT to completely reanneal and migrate as streptavidin-bound dsDNA on a nondenaturing gel (data not shown).

In the absence of streptavidin, the unwinding of DNA substrates was unchanged whether the biotin moiety was on the 5′-to-3′ or the 3′-to-5′ strand of the duplex DNA (Figure 5B; open circles and squares, respectively). In addition, the presence of the biotin moiety did not affect DNA unwinding (data not shown). The presence of streptavidin did not change the rate of unwinding of the biotinylated 3′-to-5′ strand of the duplex DNA (Figure 5, compare open and filled squares). However, the presence of streptavidin abolished unwinding of the biotinylated 5′-to-3′ strand of duplex DNA (Figure 5, compare open and filled circles). A similar result was obtained by Raney et al. (*31*). Our results confirm the interpretation of the 3′-biotinylated DNA end results shown in Figure 4, and together these results suggest that only the 5′-to-3′ strand is encircled by the helicase during DNA unwinding while the other strand is excluded.

DISCUSSION

We varied the length of the ssDNA tails and used streptavidin-biotinylated DNA substrates to examine the mechanism of T7 DNA-catalyzed DNA unwinding. A model for T7 helicase action based on our findings is shown in Figure 6A.

While wrapping of the DNA to contact more than two subunits of the helicase is the most speculative aspect of the model (Figure 6A), it is supported by experiments where the 5′-ssDNA tail adjacent to the duplex DNA was varied. The trend was of increasing rate of DNA unwinding with increasing 5′-ssDNA tail length until the tail was 55 nucleotides (Figure 2). Fifty-five nucleotides of ssDNA is sufficient to encircle the periphery and travel through the central cavity of the helicase as depicted in Figure 6A. [This calculation is based on the common measurement of 3.4−4.5 Å ssDNA contour length/nucleotide and the 25−30 Å diameter and 90 Å depth of the central cavity of the helicase ring (*11*, *32*, *33*)]. While unlikely, it is possible that the increase in the rate of DNA unwinding is due to two helicases binding to ssDNA tail longer than 35 nucleotides. Two helicases have been found to bind ssDNA longer than 35 nucleotides; however, an interaction between these helicases was not detected (*25*, *34*). Similarly, we have varied the helicase concentration in our experiments and have failed to detect any cooperative interactions (data not shown). Furthermore, EM studies suggest that the helicase only orients in the 5′-to-3′ direction along the ssDNA. Clusters of helicases but not dodecamers were observed (*11*). If multiple helicases were able to unwind DNA faster than one helicase, the rate of DNA unwinding should have increased

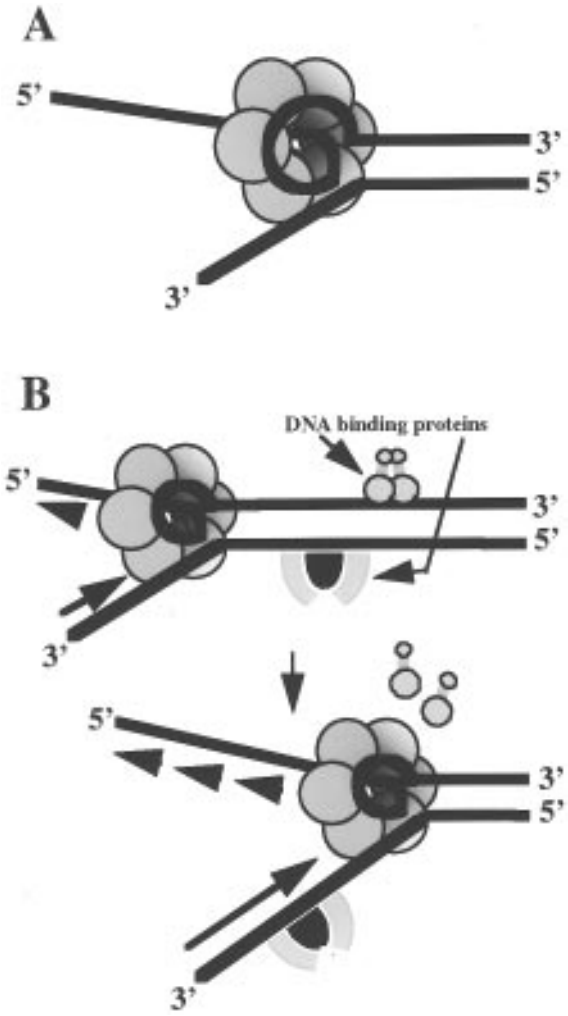

FIGURE 6: Models for T7 DNA helicase action. (A) A model for DNA unwinding by the T7 DNA helicase. The subunits of the ring-like hexameric helicase are depicted by shaded ovals. The 5′-to-3′-ssDNA strand is encircled and wrapped by the helicase. All six units of the helicase contact the DNA. Whereas, the 3′-to-5′-ssDNA tail is excluded from the central cavity during DNA unwinding. (B) A model predicting the outcome of collisions between the helicase and protein−DNA complexes during DNA replication. The leading and lagging strands during DNA replication are depicted by arrows. Proteins interacting predominantly with the lagging strand, which is represented by multiple short arrows, are stripped from the DNA. Proteins interacting predominantly with the leading strand, which is represented by one long arrow, survive collision with the helicase.

as the tail length was increased beyond 55 nucleotides (see Figure 2). In contrast, the observed slower rate seen most clearly at 70 nucleotides could be due to an inhibitory effect of a second helicase. Moreover, while DNA binding and EM studies, which are performed under conditions where nucleotide hydrolysis cannot occur, have not detected contact between the DNA and all of the subunits of the helicase, substrate requirements for DNA binding and unwinding by the helicase are different. Forked DNA is required for initation of DNA unwinding whereas only 10 nucleotides of ssDNA is required for tight DNA binding by the helicase (Figures 1−3; *8*, *25*). A model with the helicase encircling the 5′-to-3′ DNA strand but not contacting more than two subunits and excluding the 3′-to-5′ DNA strand has been previously proposed (*14*). The previous model was based solely on analysis of EM images where the ssDNA could not be directly visualized but seemed to induce an asymmetry in the center of the hexamer and the finding from the forementioned DNA binding studies that the helicase prefers ssDNA over dsDNA (*14*, *25*).

Like Matson et al. (*8*), we found that a forked DNA substrate with a 3′-$(dT)_7$ ssDNA tail was sufficient for DNA unwinding while a $(dT)_4$-tail was not. Since both tails could theoretically enter the 30-Å center of the helicase, it is likely that a DNA binding site outside the center prevents the 3′-end from entering. The finding that streptavidin bound to the 3′-end of the duplex DNA fully substitutes for this 3′-ssDNA tail suggests that only the exclusion of the 3′-to-5′ strand is essential to the mechanism of DNA unwinding and that no other interactions with this strand are needed. This finding rules out models where the primary purpose of the 3′-tail is for initial DNA binding of the helicase to the forked DNA. Two other major models for the mechanism of T7 DNA helicase-catalyzed DNA unwinding are also not favorable: (1) a "torsional" model where the subunits of the helicase bind to both ssDNA tails at the ss/ds junction and distort this region in a TTP-dependent manner, thereby causing the duplex DNA to unwind (*1*). (2) A type of rolling mechanism model where the hexamer encircling the 5′-to-3′ ssDNA tail flanking the duplex DNA provides the helicase with high processivity, but unwinding is accomplished by interactions with the 3′-to-5′ ssDNA tail and the duplex DNA (*7*). These results also suggest that the general mechanism of DNA unwinding by a hexameric helicase and the dimeric *E. coli Rep* helicase, which only requires a single ssDNA tail (*20*), may be significantly different.

How the 3′-to-5′ ssDNA strand displaced by the helicase is generated remains to be determined. The helicase could generate the 3′-to-5′ strand by capturing the 5′-to-3′ ssDNA generated by thermal "breathing" at the ss/dsDNA junction or by interacting with the dsDNA at the 5′-to-3′ ss/dsDNA junction and actively melting it.

Implications for Collisions between the Helicase and Other Proteins Interacting with the DNA. Our model for the mechanism of DNA unwinding by the T7 DNA helicase presented in Figure 6A makes certain predictions regarding the outcome of collisions between the helicase and protein−DNA complexes (less tightly associated than streptavidin and biotin) during cellular processes (such as DNA replication, DNA repair, DNA recombination, RNA transcription, and RNA splicing). During DNA replication, our model in Figure 6B predicts that proteins contacting predominantly the 5′-to-3′ strand or the lagging strand, which the helicase encircles, will be completely displaced from the DNA. Whereas, proteins contacting predominantly the 3′-to-5′ or leading DNA strand, which is excluded from the center of the helicase, could possibly survive a collision. If the proteins are a part of a larger protein complex, some DNA interactions could be disrupted while others are reformed, thereby increasing their chances of survival. Our predictions for collisions while speculative are consistent with the outcome of collisions of a DNA replication fork driven by the T4 phage gene 41 helicase and a transcribing RNA polymerase (*35*−*37*). When the RNA polymerase is transcribing the lagging DNA strand, collision and passage of the helicase-driven replication fork cause the RNA polymerase to switch to the newly replicated daughter strand (*37*). However, when the RNA polymerase is transcribing the leading strand, the RNA polymerase continues transcribing this strand after collision with and passage by the helicase-

driven replication fork (*35*−*37*). Our model is also consistent with the observation that, when a replication fork passes, three out of four nucleosomes remain on the leading strand (*38*). Lastly, it is noteworthy that on the side of *E. coli* replication termination protein, Tus, which allows replication fork passage, phosphate backbone interactions of the Tus protein are predominantly on the lagging strand (*39*). This would ensure disruption of these contacts during a collision with a helicase and thereby allow unimpeded DNA synthesis by the DNA polymerase. While these predictions need to be tested experimentally, they illustrate the general importance of understanding the mechanism of DNA helicase-catalyzed DNA unwinding.

ACKNOWLEDGMENT

We thank Dr. JoAnn Farr for technical assistance and Coleen Hacker and Dr. Bin Liu for critical reading of the manuscript.

REFERENCES

1. Lohman, T. M. (1992) *Mol. Microbiol. 6*, 5−14.
2. Matson, S. W. (1990) *Annu. Rev. Biochem. 6*, 289−329.
3. Ellis, N. A., Groden, J., Straughen, J., Ciocci, S., Proytcheva, M., and German, J. (1995) *Cell 83*, 655−666.
4. Epstein, C. J., and Motulsky, A. G. (1996) *BioEssays 18*, 1025−1027.
5. Friedberg, E. C. (1992) *Cell 71*, 887−889.
6. Lombard, D. B., and Guarente, L. (1996) *Trends Genet. 12*, 283−286.
7. Lohman, T. M., and Bjornson, K. P. (1996) *Annu. Rev. Biochem. 65*, 24509−24517.
8. Matson, S. W., Tabor, S., and Richardson, C. C. (1983) *J. Biol. Chem. 258*, 14017−14024.
9. Tabor, S., and Richardson, C. C. (1981) *Proc. Natl. Acad. Sci. U.S.A. 78*, 205−209.
10. Dunn, J. J., and Studier, F. W. (1983) *J. Mol. Biol. 166*, 477−535.
11. Egelman, E. H., Yu, X., Wild, R., Hingorani, M. M., and Patel, S. S. (1995) *Proc. Natl. Acad. Sci. U.S.A. 92*, 3869−3873.
12. San Martin, M. C., Stamford, N. P. J., Dammerova, N., Dixon, N. E., and Carazo, J. M. (1995) *J. Struct. Biol. 114*, 167−176.
13. Stasiak, A., Tsaneva, I. R., West, S. C., Benson, C. J. B., Yu, X., and Egelman, E. H. (1994) *Proc. Natl. Acad. Sci. U.S.A. 91*, 7618−7622.
14. Yu, X., Hingorani, M. M., Patel, S. S., and Egelman, E. H. (1996) *Nature Struct. Biol. 3*, 740−743.
15. Yu, X., Jezewska, M. J., Bujalowski, W., and Egelman, E. H. (1996) *J. Mol. Biol. 259*, 7−14.
16. Matson, S. W., and Richardson, C. C. (1983) *J. Biol. Chem. 258*, 14009−14016.
17. Patel, S. S., Rosenberg, A. H., Studier, W., and Johnson, K. A. (1992) *J. Biol. Chem. 267*, 15013−15021.
18. Abrahams, J. P., Lesile, A. G. W., Lutter, R., and Walker, J. E. (1994) *Nature 370*, 621−628.
19. Washington, M. T., Rosenberg, A. H., Griffin, K., Studier, F. W., and Patel, S. S. (1996) *J. Biol. Chem. 271*, 26825−26834.
20. Amaratunga, M., and Lohman, T. M. (1993) *Biochemistry 32*, 6815−6820.
21. Sambrook, J., Fritsch, E. F., and Maniatis, T. (1989) *Molecular Cloning: A Laboratory Manual*, Cold Spring Harbor Laboratory, Cold Spring Harbor, NY.
22. Sano, T. S., Pandori, M. W., Chen, X., Smith, C. L., and Cantor, C. R. (1995) *J. Biol. Chem. 270*, 28204−28209.
23. Dong, F., Gogol, E. P., and von Hippel, P. H. (1995) *J. Biol. Chem. 270*, 7462−7473.
24. Yuzhakov, A., Turner, J., and O'Donnell, M. (1996) *Cell 86*, 877−886.
25. Hingorani, M. M., and Patel, S. S. (1993) *Biochemistry 32*, 12478−12487.
26. Green, N. M. (1975) *Adv. Protein Chem. 29*, 85−133.
27. Hendrickson, W. A., Pahler, A., Smith, J. L., Satow, Y., Merritt, E. A., and Phizackerley, R. P. (1989) *Proc. Natl. Acad. Sci. U.S.A. 86*, 2190−2194.
28. Weber, P. C., Ohlendorf, D. H., Wendoloski, J. J., and Salemme, F. R. (1989) *Science 243*, 85−88.
29. Iezzoni, J. C., Kang, J. H., Monotone, K. T., Reed, J. A., and Brigati, D. J. (1992) *Nucleic Acid Res. 20*, 1149−1150.
30. Yong, Y. Q., and Romano, L. J. (1996) *Chem. Res. Toxicol. 9*, 179−187.
31. Raney, K. D., Carver, T. E., and Benkovic, S. J. (1996) *J. Biol. Chem. 271*, 14074−14081.
32. Record, M. T., Jr., Woodbury, C. P., and Lohman, T. M. (1976) *Biopolymers 15*, 893−915.
33. Record, M. T., Jr. (1975) *Biopolymers 14*, 2137−2158.
34. Yong, Y., and Romano, L. J. (1995) *J. Biol. Chem. 270*, 24509−24517.
35. Liu, B., Wong, M. L., Tinker, R. L., Geiduschek, E. P., and Alberts, B. M. (1993) *Nature 366*, 33−39.
36. Liu, B., Wong, M. L., and Alberts, B. M. (1994) *Proc. Natl. Acad. Sci. U.S.A. 91*, 10660−10664.
37. Liu, B., and Alberts, B. M. (1995) *Science 267*, 1131−1137.
38. Bonne-Andrea, C., Wong, M. L., and Alberts, B. M. (1990) *Nature 343*, 719−726.
39. Kamada, K., Horiuchi, T., Ohsumi, K., Shimamoto, N., and Morikawa, K. (1996) *Nature 383*, 598−603.

BI971644V